Available online at www.sciencedirect.com
ScienceDirect
Trans. Nonferrous Met. Soc. China 30(2020) 1046−1057
Transactions of Nonferrous Metals Society of China
www.tnmsc.cn

Influence of Ni^{2+}/Co^{2+} ratio in electrolyte on morphology, structure and magnetic properties of electrolytically produced Ni−Co alloy powders

Vesna M. MAKSIMOVIĆ[1], Vladan B. KUSIGERSKI[1],
Milovan M. STOILJKOVIĆ[1], Jelena R. MALETAŠKIĆ[1,2], Nebojša D. NIKOLIĆ[3]

1. Institute of Nuclear Sciences, "Vinča", University of Belgrade, P. O. Box 522, Belgrade 11001, Serbia;
2. Laboratory for Advanced Nuclear Energy, Institute of Innovative Research,
Tokyo Institute of Technology, 2-12-1 Ookayama, Meguro-ku, Tokyo 152-8550, Japan;
3. ICTM-Department of Electrochemistry, University of Belgrade,
Njegoševa 12, P. O. Box 473, Belgrade 11001, Serbia

Received 27 August 2019; accepted 4 March 2020

Abstract: Nickel−cobalt (Ni−Co) alloy powders were produced galvanostatically by using sulphate electrolytes with various ratios of Ni^{2+}/Co^{2+} (mole ratios). The morphology, phase structure, chemical composition and magnetic properties were examined by scanning electron microscope (SEM), X-ray diffractometer (XRD), atomic emission spectrometer (AES), and SQUID-based magnetometer, respectively. Morphology of the particles changed from cauliflower-like and dendritic to coral-like and spongy-like ones with increasing Ni^{2+}/Co^{2+} ratio from 0.25 to 4.0. XRD analysis of the Ni−Co powders revealed that the decrease of Ni^{2+}/Co^{2+} ratios (the increase of Co content) caused a change of structure from face centered cubic (FCC) obtained for the ratios of 4.0, 1.5 and 0.67 to a mixture of FCC and hexagonal closed-packed (HCP) phases for the ratio of 0.25. The increasing content of nickel led to change of mechanism of electrolysis from irregular (up to ~40 wt.% Ni in the electrolytes) to close to equilibrium (between ~40 and 60 wt.% Ni in the electrolytes) and anomalous co-deposition (over 60 wt.% Ni in the electrolytes) type. All of the obtained Ni−Co alloy samples behaved as soft magnetic materials while their magnetic parameters showed immediate composition dependence since both coercivity and saturation magnetization almost linearly increased with increase of the Co content.

Key words: Ni−Co alloy powders; electrolysis; hydrogen; morphology; magnetic properties

1 Introduction

Thinking to unique characteristics, such as high mechanical strength, good wear resistance, anticorrosive performance, thermal conductivity, thermal stability, electrical conductivity, electro-catalytic activity, and specific magnetic properties, nickel−cobalt (Ni−Co) alloys attract a huge attention of both academic and technological communities [1,2]. Various methods are used for the synthesis of Ni−Co alloys, such as electro-deposition [3−6], sol−gel method [7,8], co-precipitation [1,9], and solvothermal treatment [10]. The application of Ni−Co alloys is closely associated with their morphological characteristics that are in turn dependent on method and conditions of synthesis. Depending on method and conditions of synthesis, Ni−Co alloys can be obtained either in the compact form [3] or in various disperse forms, such as icosahedral nanocrystals [8], coral-like [1], cubic-like [9], fibrous [9,11], and other fine powder shapes [7].

The investigation of the electrodeposition processes in the hydrogen co-deposition range is very important, and electrodeposition processes

Corresponding author: Nebojša D. NIKOLIĆ; E-mail: nnikolic@tmf.bg.ac.rs
DOI: 10.1016/S1003-6326(20)65276-1

are a feature of metals characterized by medium and low values of both the exchange current density and overpotential for hydrogen discharge [12,13]. Metals with these characteristics are denoted as either intermediate (Cu, Ag (complex electrolytes), Au) or inert (Ni, Co, Fe, Pt, Pd) metals [14]. One main benefit of using electrodeposition processes with parallel hydrogen evolution is the formation of deposits with very high surface area and nanostructural characteristics, such as the honeycomb-like [12,13,15,16] or the 3D (three-dimensional) foam [12,13,17] structures. The main characteristics of these deposits are holes or pores formed by the detachment of hydrogen bubbles surrounded by cauliflower-like or dendritic particles. Almost all metals from the intermediate and inert groups are formed in the honeycomb-like or the 3D foam forms, e.g. Cu [12,13,15−19], Ag [20], Au [21], Ni [22], Pd [23], and Pt [24]. Aside from pure metals, some technological important alloys, such as Cu−Sn [25], Ni−Cu [26] and Ni−Co [27] are also formed in this form.

Depending on the quantity of evolved hydrogen during electrodeposition process, the typical forms of powder particles obtained after removing the deposits from the electrode surface are: dendrites, cauliflower-like and spongy-like particles [12]. The cauliflower-like particles are obtained by removing the deposit from the honeycomb-like structures [28−30], while dendrites and spongy-like particles are formed by a native electrodeposition process. These forms of particles are observed among powder particles of all above mentioned pure metals [12].

The fact that both metals make Ni−Co alloys belong to the group of inert metals clearly indicates that appearing of hydrogen evolution as a parallel reaction plays a crucial role in the formation of Ni−Co powders by electrolysis processes. Investigations on the formation of Ni−Co alloy in the powder form were mainly initiated in the last decade [31−36]. The typical forms of powder particles obtained by eletrodeposition of this alloy at a very high current density of 500 mA/cm^2 were identified as dendrites and the spongy-like ones, and it was shown that the shape of these particles did not depend on the electrolyte type [31−33]. Unlike the type of electrolyte, a structure of the used substrate for electrodeposition had a strong effect on the morphology of Ni−Co disperse deposits [34]. Simultaneously, increasing the current density of electrodeposition led to a ramification of Ni−Co dendrites and high ordered dendrites with secondary branches can be formed.

Electrodeposition of the binary Ni−Co system has been studied comprehensively, mainly due to its importance in the soft magnetism field [37,38]. The possibility to obtain different nanostructures and/or morphologies provides an excellent opportunity for establishing correlations between structure and magnetism of these alloys, and consequently to tailor their magnetic properties. Another reason for the interest in this system is that the deposition of Ni−Co alloys demonstrates the phenomenon of anomalous co-deposition [39] and based on the binary-phase diagram builds series of solid solutions in the whole range of concentrations.

Using well known knowledge about the influence of hydrogen on the electrodeposition processes, this work primarily dealt with the role of hydrogen in creating of the final morphology of Ni−Co powder particles. In this case, this was caused by the fact that electrodeposition processes of Ni, Co or Ni−Co catalyzed the reaction of hydrogen evolution [31]. Formation of hydrogen bubbles at high current density represented the rate limiting step of the electrochemical process, where the current of hydrogen evolution reached 80%−85% of the overall current in the case of Co, and even 90% in the case of Ni. This further caused the dependence of the amount of evolved hydrogen on Ni^{2+}/Co^{2+} ratios (mole ratios) [31], with strong consequences on morphology of the powder particles. In this study, the electrolysis processes were performed at a moderate current density of 100 mA/cm^2 from sulphate electrolytes with various Ni^{2+}/Co^{2+} ratios in the initial electrolytes. As expected, the amount of evolved hydrogen at this current density was smaller than that at 500 mA/cm^2 [31], indicating the formation of some novel shapes of Ni−Co particles in this investigation. The formation mechanism of all observed particles was explained. It was shown that the morphology of powder particles strongly depended on the Ni^{2+}/Co^{2+} ratio in the initial electrolyte. Also, the microstructure, chemical and phase compositions and magnetic properties of the Ni−Co alloy powders were compared systematically and mutually correlated with morphology of synthesized particles.

2 Experimental

All alloy powder samples were electrodeposited at the room temperature in a cylindrical glass cell of a total volume of 1 dm^3. Working electrode was a glassy carbon (GC) rod of the diameter of 5 mm with the total surface area of 7.5 cm^2 which was immersed in the electrolyte and placed in the middle of the cell. Cylindrical nickel foil placed close to the cell walls was used as a counter electrode providing excellent current distribution in the cell. Electrodeposition of powders was performed with a constant current regime at a current density of 100 mA/cm^2 using appropriate power supply. The deposition time was 120 min. The amount of electrodeposited powders was sufficient for further analysis. Ni−Co powders were electrodeposited from the electrolyte containing 1 mol/L $(NH_4)_2SO_4$, 0.7 mol/L NH_4OH, and nickel and cobalt sulfate salts with the following ratios:

(1) Ni^{2+}/Co^{2+}=4.0
(0.1 mol/L $NiSO_4$/0.025 mol/L $CoSO_4$);
(2) Ni^{2+}/Co^{2+}=1.5
(0.06 mol/L $NiSO_4$/0.04 mol/L $CoSO_4$);
(3) Ni^{2+}/Co^{2+}=0.67
(0.04 mol/L $NiSO_4$/0.06 mol/L $CoSO_4$);
(4) Ni^{2+}/Co^{2+}=0.25
(0.025 mol/L $NiSO_4$/0.1 mol/L $CoSO_4$).

pH value of the electrolytes was 9.3±0.20. After deposition, powders were washed with EASY pure UV water and alcohol and dried in the air.

The morphology, phase structure, and chemical composition of the produced powders were investigated using scanning electron microscopy (SEM), X-ray diffractometry (XRD) and atomic emission spectrometry (AES), respectively. For morphological analysis of the powders, SEM models JEOL JSM−6460LV and Philips XL30 were used. The XRD analysis of Ni−Co powders was performed by Rigaku Ultima IV equipment using Ni-filtered Cu K_α radiation operating at 40 kV and 40 mA. XRD patterns were scanned in the 2θ range between 30° and 100° with a step of 0.02°. The unit cell parameters and fractions of the phases were calculated by using the software package Powder Cell [40]. Chemical analysis of the powders was performed using SPECTRO ICP−OES 17.5 MHz spectrometer (in the further text ICP−OES). Samples for the analysis of about 50 mg were dissolved in 5 mL HCl (1:1) at slightly elevated temperature.

Measurements of the field dependence of isothermal magnetization at room temperature for all the samples were performed on a commercial SQUID-based magnetometer Quantum Design MPMS XL−5, in a field range of ±5 T.

3 Results and discussion

3.1 Morphology

Figures 1−4 show morphologies of Ni−Co

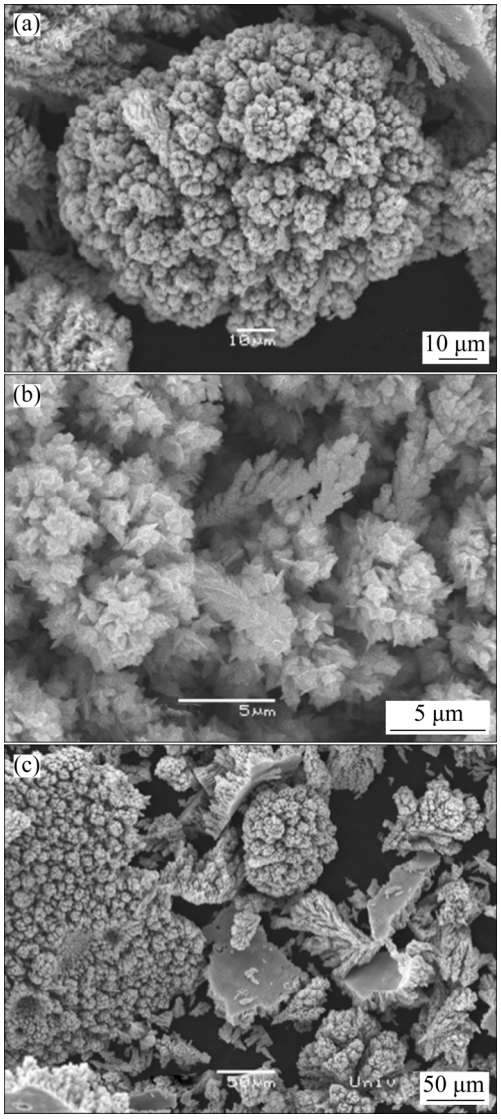

Fig. 1 Morphologies of Ni−Co powder particles obtained at current density of 100 mA/cm^2 with Ni^{2+}/Co^{2+} ratio of 0.25 in initial electrolyte: (a) Cauliflower-like particle; (b) Dendritic particles; (c) Holes formed from detached hydrogen bubbles

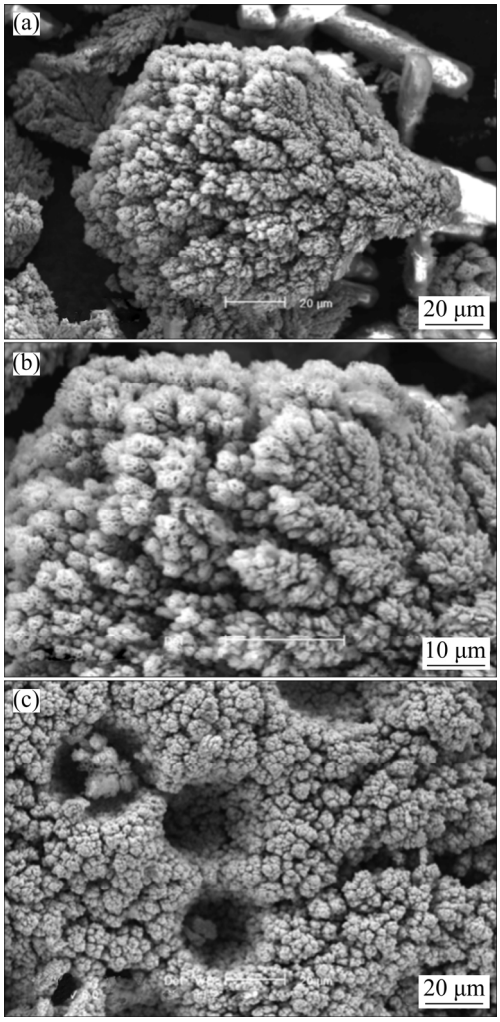

Fig. 2 Morphologies of Ni−Co powder particles obtained at current density of 100 mA/cm^2 with Ni^{2+}/Co^{2+} ratio of 0.67 in initial electrolyte: (a) Degenerate dendrite; (b) Tops of particle shown in Fig. 2(a); (c) Holes formed from detached hydrogen bubbles surrounded by relatively compact cauliflower-like agglomerates of grains

powder particles obtained at a current density of 100 mA/cm^2 for various ratios of Ni^{2+}/Co^{2+} in initial electrolytes: 0.25 (Fig. 1), 0.67 (Fig. 2), 1.5 (Fig. 3) and 4.0 (Fig. 4). Figure 1 reveals the dominant presence of two types of particles obtained with the Ni^{2+}/Co^{2+} ratio of 0.25: cauliflower-like (Fig. 1(a)) and dendritic (Fig. 1(b)) ones. Aside from these particles, individual holes originating from the detached hydrogen bubbles can be also detected in a structure of powder particles obtained with the ratio of 0.25 (Fig. 1(c)).

The increase of Ni^{2+}/Co^{2+} ratio from 0.25 to 0.67 had the following consequences on the morphology of powder particles: inhibition of the dendritic growth (Fig. 2(a)) followed by appearing of small holes at tops of the obtained degenerate dendritic particles (Fig. 2(b)). Simultaneously, the number of holes formed from the detached hydrogen

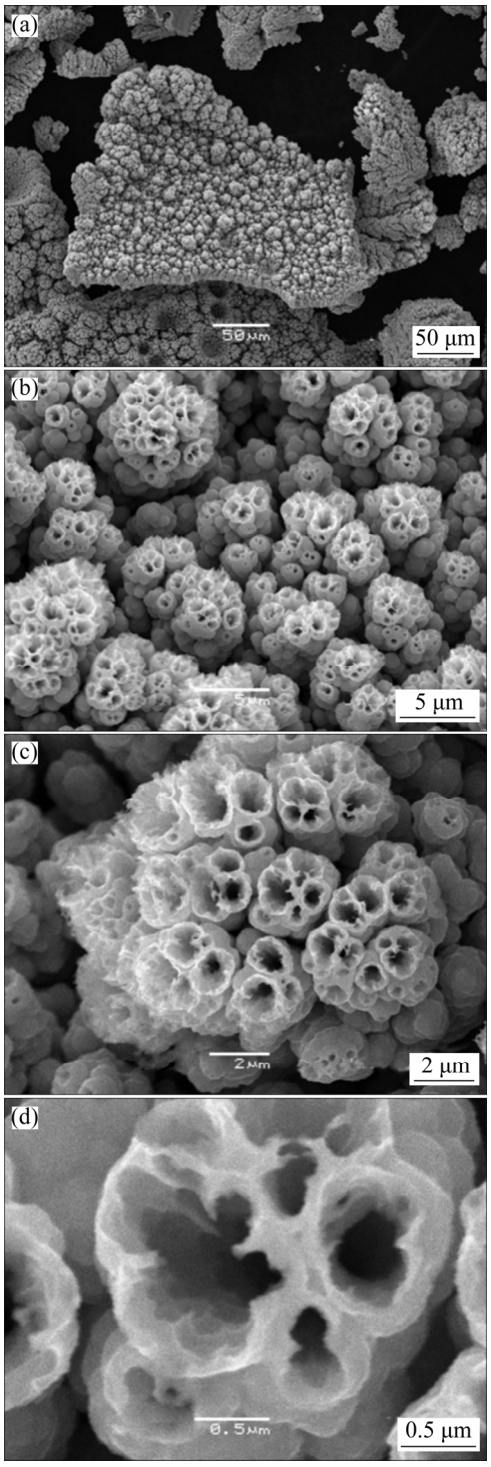

Fig. 3 Morphologies of Ni−Co powder particles obtained at current density of 100 mA/cm^2 with Ni^{2+}/Co^{2+} ratio of 1.5 in initial electrolyte: (a) Coral-like particle; (b, c) Small agglomerates constructing coral-like structure; (d) Holes formed at top of coral-like particle

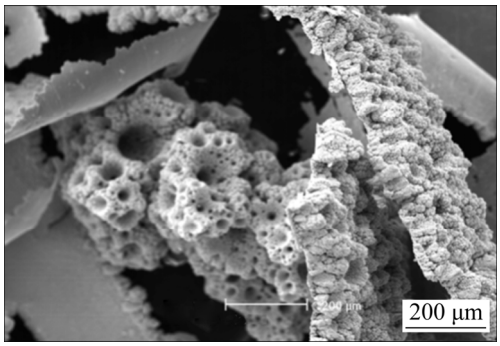

Fig. 4 Morphology of spongy-like Ni−Co powder particle obtained at current density of 100 mA/cm^2 with Ni^{2+}/Co^{2+} ratio of 4.0 in initial electrolyte

bubbles increased in relation to the ratio of 0.25. The holes were mutually separated by small relatively compact cauliflower- like agglomerates of grains, as seen in Fig. 2(c).

Further increase in Ni^{2+}/Co^{2+} ratio caused a complete inhibition of dendritic growth, as shown in Fig. 3(a). Analysis of the particle presented in Fig. 3(a) at the high magnifications shows that it consists of small agglomerates of grains (Figs. 3(b) and (c)). The open structure of these agglomerates is a result of hydrogen evolution reaction as a parallel reaction to alloy electrodeposition, and these small holes are also the consequence of detached hydrogen bubbles. The size of these small holes is about 500 nm or less, as shown in Fig. 3(d). These particles can be denoted as coral-like, and it is noteworthy to note that this type of particle has been observed for the first time in this investigation. Simultaneously, the presence of the large holes formed from the detached hydrogen bubbles surrounded by relatively compact cauliflower-like agglomerates is also detected in a structure of the powder particles obtained with Ni^{2+}/Co^{2+} ratio of 1.5 (Fig. 3(a)).

Finally, the powder particle obtained with Ni^{2+}/Co^{2+} ratio of 4.0 has the typical honeycomb-like structure (Fig. 4). The basic characteristics of this structure are holes formed from the detached hydrogen bubbles and cauliflower-like agglomerates of grains formed around them. In Ref. [31], this type of particle is often referred as spongy-like one.

3.2 Phase structure and chemical composition

The phase structure of deposited alloy powders was studied by the XRD analysis. All the structure information was taken from American Mineralogist Crystal Data Structure Base (AMCDSB) [41]. As shown in Fig. 5, when the Ni^{2+}/Co^{2+} ratio is 4.0, the XRD pattern of alloy powders shows peaks at $2\theta = 44.46°$, 51.62° and 76.24°, which correspond to (111), (200) and (220) planes of Ni−Co alloy with a face centered cubic (FCC) structure [42,43]. Their positions are slightly higher than those of pure FCC Co (44.22°, 51.52° and 75.86°) (JCPDS No. 15−0806) and slightly lower than those of pure FCC Ni (44.51°, 51.85° and 76.37°) (JCPDS No. 04−0850). The XRD data (Fig. 5) show that Ni−Co alloy powders form solid solutions and that the powders display the structure change progressively with the increase of the concentration of bath, namely the Ni^{2+}/Co^{2+} ratio. When the Ni^{2+}/Co^{2+} ratios are 0.67, 1.5 and 4.0, the powders have a single phase of FCC structure. With the increase of cobalt content and the decrease of the Ni^{2+}/Co^{2+} ratio lower than 0.67 (actually 0.25) the hexagonal closed packed (HCP) phase appears, and the structure of the deposit changes from FCC to a mixture of FCC phase and HCP phase. The characteristic reflections corresponding to HCP phase can be observed at $2\theta = 41.72°$ and 47.63° (JCPDS No. 05−0727). This result is in line with expectations, because pure Ni is FCC in equilibrium, and can dissolve substantial quantities

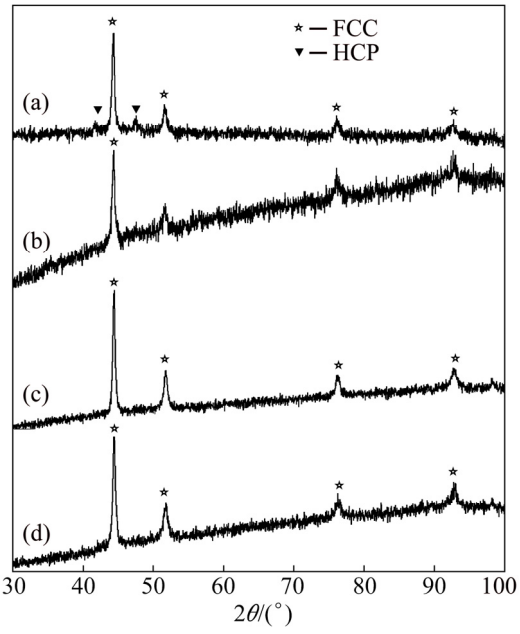

Fig. 5 XRD patterns of Ni−Co powder particles deposited from electrolytes with different Ni^{2+}/Co^{2+} ratios: (a) 0.25; (b) 0.67; (c) 1.5; (d) 4.0

of Co (up to 60 wt.% at the room temperature) [44]. The XRD pattern of samples exhibits very diffuse diffraction lines indicating small crystallite size (about 20 nm) and/or strain.

According to the results of the chemical analysis of electrodeposited powders performed by ICP−OES, the ratio of Ni^{2+}/Co^{2+}, i.e. the electrolyte composition, significantly influenced the composition of electrodeposited powders. The results are given in Table 1.

The content of Co increases, while the content of Ni decreases with the decrease of Ni^{2+}/Co^{2+} ratio in electrolyte. According to Brener's classification in Ref. [39], the behavior presented in Fig. 6 indicates three types of alloy powder co-deposition: irregular, up to 40 wt.% Ni in the solution, close to equilibrium between 40 and 60 wt.% Ni and anomalous at higher content of Ni (higher than 60 wt.% Ni). Similar behavior was noticed during the electrodeposition from the same electrolytes at a current density of 500 mA/cm^2 [32].

The irregular co-deposition is expected to occur in the system in which the standard potentials of metals are close together and with metals that form solid solution. Both conditions are met for the binary Ni−Co system [32,39]. On the other hand, it is well-known that from simple salt containing electrolytes, co-deposition of Ni and Co possesses anomalous character [32,33,39], as well as in the electrolyte containing metal complexes [32,45]. It is characterized by the anomaly that the less noble metal deposits preferentially. It is frequently associated with the electrodeposition of alloys containing one or three metals of the iron group, i.e. Fe, Co and Ni. In our case, the mixture of cauliflower-like and dendritic particles is formed by irregular type of co-deposition, while the spongy-like particles are formed by anomalous type of co-deposition.

Equilibrium co-deposition occurs from a solution which is in chemical equilibrium with both of the parent metals. Only a few examples of equilibrium alloys such as Pb−Sn and Cu−Bi are known [39]. The phenomenon of apparent equilibrium co-deposition of Ni−Co alloy powders from dilute sulphate baths was mentioned in the work of ABD EL-HALIM [46] and explained that under appropriate conditions, the regular electrodeposition of Ni−Co alloy has the same characteristic of equilibrium co-deposition with respect to relation between the deposit and bath compositions. The novel coral-like type of the particles is formed by close to equilibrium type of co-deposition, indicating that this particle type represents a transient form between classical cauliflower-like and the spongy-like particles.

The FCC structure (100%) is obtained for Ni−Co alloy powders when the content of Co is less than 61 wt.% and the mixture (FCC (90%) + HCP (10%)) is obtained in the case when the content of Co in the powder is more than 61 wt.% (Table 1). Using the XRD data, the variation of the lattice parameter of FCC Ni−Co alloy powder composition was evaluated, and results are illustrated in Fig. 7. It is obvious that the lattice parameter of FCC phase in Ni−Co alloy powders exhibits a good linear relationship with Co content. Such a trend indicates that the mutual alloying of Ni and Co dictates the formation of perfect solid solution for any composition of Ni−Co.

3.3 Magnetic properties

Field dependence of isothermal magnetization recorded at room temperature for all the samples is shown in Fig. 8. It can be seen that all curves show saturation at relatively small fields as well as low coercivity values, and both properties are typical of soft magnetic materials.

Values of saturation magnetization M_S and coercive field H_C are determined from the measured curves and plotted in Fig. 9 against the Ni/Co ratio in the powder determined from ICP-OES data, as

Table 1 Chemical compositions and crystal structures of electrodeposited powders

Sample No.	Ni^{2+}/Co^{2+} ratio in electrolyte	Co content in powder/wt.%	Ni/Co ratio in powder	Crystal structure	Lattice parameter of FCC, a/Å
1	4.0	29.8±0.7	2.48±0.08	FCC (100%)	3.5278(1)
2	1.5	36±1	2.00±0.1	FCC (100%)	3.5282(2)
3	0.67	58±2	0.78±0.06	FCC (100%)	3.5315(1)
4	0.25	61±2	0.74±0.06	FCC (90%)+HCP (10%)	3.5317(1)

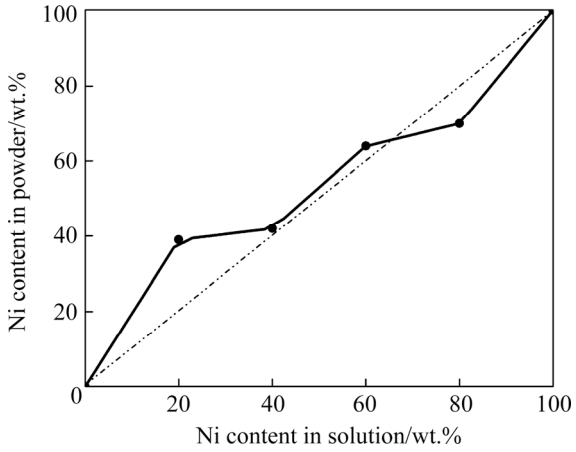

Fig. 6 Irregular, close to equilibrium and anomalous co-deposition of Ni−Co alloy powders

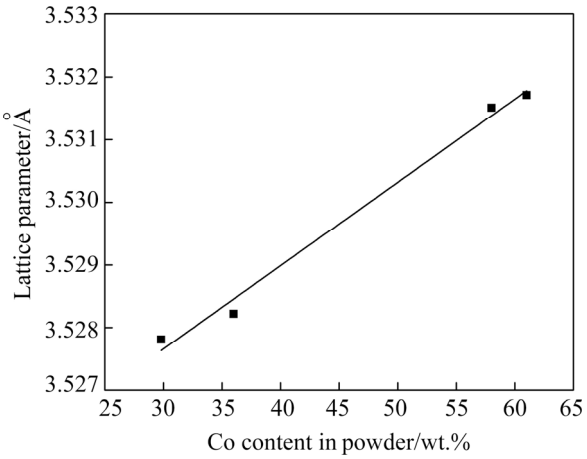

Fig. 7 Composition dependence of lattice parameter of FCC phase in Ni−Co alloy powders

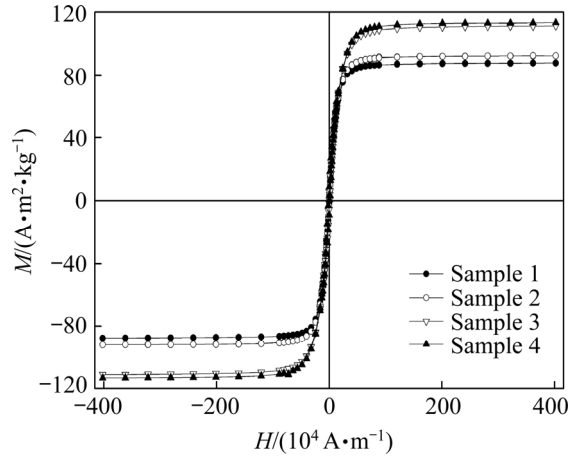

Fig. 8 Isothermal magnetization curves of samples recorded at room temperature

given in Table 1. The M_S values calculated by using the relation of Eq. (1) are also plotted in Fig. 9.

$$M_S=M_S(\text{Co})\cdot x+M_S(\text{Ni})\cdot(1-x) \quad (1)$$

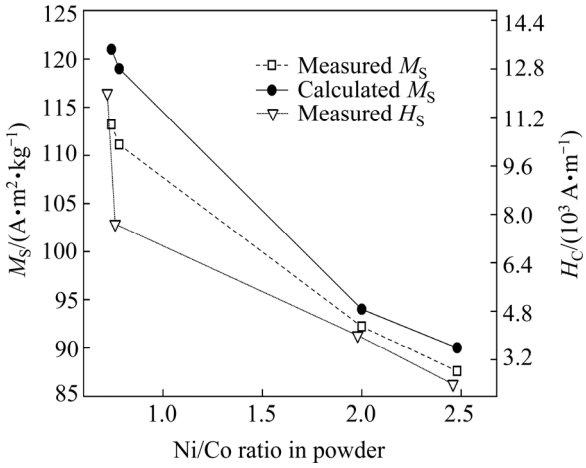

Fig. 9 Values of coercive field H_C and saturation magnetization M_S obtained from measured hysteresis curves and calculated values of saturation magnetization obtained by applying Eq. (1)

where x denotes cobalt content, while M_S(Co) and M_S(Ni) represent saturation magnetization values of Co and Ni metals, respectively [47]. According to Ref. [48], these values were considered to be 168 and 58 A·m^2/kg for Co and Ni, respectively.

By inspecting Fig. 9, several conclusions could be made. With the increase of cobalt content, values of saturation magnetization also increase, which is expected since saturation magnetization of cobalt is considerably higher than that for nickel, as already mentioned. One can see that the calculated values of M_S closely follow the experimental values, which means that the ratios of Ni/Co determined from ICP−OES data are credible. Slightly lower values of experimentally obtained M_S values could be explained by the prospective presence of metal oxides which usually form on the metal surface. Since both NiO and CoO oxides are antiferromagnetic [48], their contribution to the overall magnetization is almost negligible compared to the values of the corresponding ferromagnetic metals.

The obtained values of coercive fields H_C also increase with the increase of the cobalt content, which is expected since anisotropy of cobalt ion is considerably higher in comparison with other 3d metal ions due to the incomplete freezing of its orbital momentum [49]. It could be easily seen that H_C values increase almost linearly with cobalt content for samples 1−3, while the significant jump is obtained for sample 4 which has the highest content of cobalt (≈61 wt.%). For this sample, XRD

data analysis pointed to the presence of two crystal phases, namely FCC and HCP phases, which is in line with the literature data on the stability of the nickel FCC phase up to the 60% of dissolved cobalt [44]. At the same time, it is well known that HCP-Co is magnetically much harder than FCC-Co, meaning that the coercive field H_C^{HCP} can be up to an order of magnitude higher than H_C^{FCC} while saturation magnetization values of both phases are virtually the same [48]. Thus, the jump in the coercive field value with the constant increase of saturation magnetization could be explained by the formation of HCP-Co phase in cobalt-rich sample 4 (Ni^{2+}/Co^{2+}=0.25).

3.4 General discussion of presented results

In the dependence of Ni^{2+}/Co^{2+} ratio, three main types of surface morphologies are observed: dendrites, the coral-like and spongy-like particles. With increasing the Ni^{2+}/Co^{2+} ratio, the morphology of powder particles changed from dendrites to the spongy-like particles (Figs. 1–4). At the first sight, it is clear that the shape of observed particles is determined by hydrogen evolution as parallel reaction to alloy electrodeposition, with a tendency of increasing quantity of evolved hydrogen with the increasing Ni^{2+}/Co^{2+} ratio. Hydrogen generated during an electrodeposition process caused a stirring of the electrolyte in the near-electrode layer, leading to a decrease in the thickness of the diffusion layer, an increase in the limiting diffusion current density and a decrease in the degree of diffusion control of the electrodeposition process [15]. It can be concluded by the analysis of the surface morphologies that effectiveness of solution stirring by evolved hydrogen increased with increase of Ni^{2+}/Co^{2+} ratio. Then, the change of surface morphology from dendrites to spongy-like particles can be explained in the following way: simultaneous formation of the cauliflower-like particles, dendrites and individual holes at 100 mA/cm^2 with the Ni^{2+}/Co^{2+} ratio of 0.25 (Fig. 1) makes the electrode surface during the deposition process very non-uniform, indicating that the diffusion layer of the macroelectrode was not disrupted [16]. This meant that hydrogen evolution was not vigorous enough to achieve any significant effect on stirring of the electrolyte, and hence, on the hydrodynamic conditions in the near-electrode layer. The effect of generated hydrogen on the hydrodynamic conditions in the near-electrode layer becomes visible at the same current density with the Ni^{2+}/Co^{2+} ratio of 0.67 (Fig. 2). As a result of enhanced stirring of the electrolyte in the near-electrode layer caused by intensification of hydrogen evolution, the growth of dendrites was inhibited. Simultaneously, the small holes were formed at the tops of the inhibited particles (often denoted as cauliflower-like ones), and larger number of holes in the relation to the Ni^{2+}/Co^{2+} ratio of 0.25 were observed. The presence of a channel structure in cauliflower-like particles was also clearly seen (Fig. 2(a)). The effectiveness of a solution stirring in the near-electrode layer by evolved hydrogen further increased with increasing Ni^{2+}/Co^{2+} ratio (Fig. 3). The complete inhibition of the growth of dendrites and formation of cauliflower-like particles with the hole structure on the grains (these small particles with holes constructing the large cauliflower-like particle are further denoted by coral-like ones to distinguish from the classical cauliflower-like particles) are caused by further intensification of hydrogen evolution and its consequence on the morphology of powder particles. As result of the further intensification of hydrogen evolution reaction, the spongy-like particles consisting of holes formed from the detached hydrogen bubbles surrounded by compact cauliflower-like agglomerates occurred with the Ni^{2+}/Co^{2+} ratio of 4.0 (Fig. 4).

Hence, the morphology of powder particles is exclusively determined by the amount of produced hydrogen and by its effect on the hydrodynamic conditions in the near-electrode layer. It is clear that the formation of these particles can be explained by the concept of “effective overpotential” or “effective potential” [12,50]. According to this concept, in the conditions of vigorous hydrogen evolution, the electrodeposition process occurs at an overpotential or potential which is effectively lower than that specified, and this overpotential (potential) is denoted as “effective” in a deposition process. Then, the morphologies of metal deposits become similar to those obtained at some lower overpotentials (potentials) at which hydrogen evolution does not occur or is very slow [15].

The decrease of potential at which electrodeposition process really occurs with increasing Ni^{2+}/Co^{2+} ratio can be confirmed by the following analysis: as already mentioned, the

cauliflower-like particles, dendrites and individual holes were formed with the Ni^{2+}/Co^{2+} ratio of 0.25 (Fig. 1). Electrodeposition process with the Ni^{2+}/Co^{2+} ratio of 0.67 characterized the absence of dendrites and formation of the cauliflower-like particles with visible channel structure through them. The fact that cauliflower-like particles are always formed at the lower potentials than dendritic ones proves that "the effective potential" with Ni^{2+}/Co^{2+} ratio of 0.67 is lower than the one for the ratio of 0.25. The similar conclusion can be also derived for other Ni^{2+}/Co^{2+} ratios. The cauliflower-like particle formed with the Ni^{2+}/Co^{2+} ratio of 1.5 (Fig. 3(a)) is more compact than that formed with the ratio of 0.67 (Fig. 2(a)), which indicates the further decrease of the potential at which deposition process really occurs. Also, it is important to note that the cauliflower-like particle obtained with the ratio of 1.5 (Fig. 3(a)) is constructed from coral-like particles, of which the basic characteristic is open structure due to small detached hydrogen bubbles (about 500 nm) (Figs. 3(b−d)). In electrodeposition processes accompanied by vigorous hydrogen evolution, the amount of hydrogen produced during deposition process is divided into the two parts [51]: the first part is spent for creating holes (those in the coral-like particles and in large holes). Hydrogen spent for creating these holes does not contribute to stirring of the electrolyte in the near-electrode layer, but only contributes to the increase of surface area of the particles. The second part represents the difference between the overall generated hydrogen and the quantity of hydrogen spent for creating holes. This difference produces a stirring of the electrolyte, and the channel structure is formed from it. The regular zone of decreased nucleation formed around the coral-like particles (Fig. 3(b)) proves more compact structure of the large particle (Fig. 3(a)) than the cauliflower-like particle formed with the ratio of 0.67 (Fig. 2(a)), confirming that "effective potential" by which this particle is formed is lower than that with the ratio of 0.67. With further increase of Ni^{2+}/Co^{2+} ratio from 1.5 to 4.0, the number of holes and the compactness of deposits around holes in the spongy-like particles are further increased. Formation of very compact agglomerates of grains with the Ni^{2+}/Co^{2+} ratio of 4.0 additionally proves that "effective potential" is lower than that with the Ni^{2+}/Co^{2+} ratio of 1.5.

The shape change of Ni−Co particles from cauliflower-like and dendritic to coral-like and spongy-like ones was accompanied by the mechanism change of their formation from irregular to close to equilibrium and anomalous type of co-deposition. Formation of the mixture of cauliflower-like and dendritic particles from the electrolyte with Co^{2+} content in the electrolyte four times larger than Ni^{2+} content (up to 40 wt.% Ni) corresponds to irregular type of co-deposition. Formation of novel type of the particles, denoted as coral-like, can be attributed to close to equilibrium type of co-deposition (between 40 and 60 wt.% Ni). Finally, the spongy-like particles are formed by anomalous type of co-deposition (above 60 wt.% Ni). These trends in change of morphology of Ni−Co particles and type of co-deposition are accompanied by intensification of hydrogen evolution reaction as parallel reaction to alloy powder electrolysis. This clearly indicates a crucial role of generated hydrogen in not only morphology of the particles, but also a mechanism of their formation. Simultaneously, decreasing Co^{2+} content in the electrolyte leads to a crystal structure change of the produced powder particles. With the increasing Ni^{2+}/Co^{2+} ratio, a crystal structure change from the mixture of face centered cubic (FCC) and hexagonal closed-packed (HCP) phases to face FCC phase is observed. Results of magnetic measurements are also in an excellent agreement with the Ni^{2+}/Co^{2+} ratios, proving the strong influence of the Ni^{2+}/Co^{2+} ratios in the initial electrolytes not only on the morphology and structure, but also on the magnetic characteristics of electrolytically produced Ni−Co powder particles.

4 Conclusions

(1) Depending on Ni^{2+}/Co^{2+} ratio, the following dominant types of particles are formed at a current density of 100 mA/cm^2: cauliflower-like and dendrites (with Ni^{2+}/Co^{2+} ratio of 0.25), coral-like (with Ni^{2+}/Co^{2+} ratio of 1.5) and spongy-like (with Ni^{2+}/Co^{2+} ratio of 4.0) particles. Morphological analysis of the obtained particles indicates that the change of their morphology with increasing Ni^{2+}/Co^{2+} ratio is a result of intensification of hydrogen evolution as a parallel reaction.

(2) XRD data show that solid solution of Ni−Co alloy powder is formed and the phase

component changes progressively under different electrolyte compositions. With low Co content, the powder alloys exhibit single phase of FCC structure. When the content of Co is above 61 wt.%, the alloy powder is composed of mixture of FCC and HCP phases.

(3) Three types of co-deposition in the Ni−Co systems are detected: irregular, close to equilibrium and anomalous. The mixture of cauliflower-like and dendritic particles is formed by irregular type of co-deposition. The close to equilibrium type is responsible for the formation of coral-like particles. The spongy-like particles are formed by anomalous type of co-deposition.

(4) Ni−Co alloy samples possess properties of soft magnetic materials like saturation in a small applied fields and low coercive field values. Both saturation magnetization and coercivity increase almost linearly with Co content which is expected due to the significantly higher values of both parameters for cobalt in comparison to nickel. Jump in coercive field value for sample with the highest content of cobalt is explained by the formation of HCP-Co phase which is magnetically much harder than the FCC-Co phase.

Acknowledgments

This work was financially supported by the Ministry of Education, Science and Technological Development of the Republic of Serbia through the Project Nos. III45012, 172019 and III45015.

References

[1] HU Ping, CHEN Zhen-yu, CHANG Tian, DENG Jie, YANG Fan, WANG Kuai-she, LI Qing-wei, HU Bo-liang, YU Hai-liang, WANG Wen-peng. Magnetic properties of the nanoscale coral-shaped Ni−Co alloy powder with different Co contents [J]. Journal of Alloy and Compound, 2017, 727: 332−337.

[2] LUPI C, DELL'ERA A, PASQUALI M. Nickel–cobalt electrodeposited alloys for hydrogen evolution in alkaline media [J]. International Journal of Hydrogen Energy, 2009, 34: 2101−2106.

[3] HAGAROVÁ M, JAKUBÉCZYOVÁ D, CERVOVÁ J. Microstructure and properties of electroplated Ni−Co alloy coatings [J]. International Journal of Electrochemical Science, 2015, 10: 9968−9974.

[4] ZHOU Ke-chao, MA Li, LI Zhi-you. Oxidation behaviors of electrodeposited nickel−cobalt coatings in air at 960 °C [J]. Transactions of Nonferrous Metals Society of China, 2011, 21: 1052−1060.

[5] SEKAR R, JAGADESH K K, RAMESH BAPU G N K. Development of black Ni−Co alloy films from modified Watts electrolyte and its morphology and structural characteristics [J]. Transactions of Nonferrous Metals Society of China, 2015, 25: 1961−1967.

[6] ZAMANI M, AMADEH A, LARI BAGHAL S M. Effect of Co content on electrodeposition mechanism and mechanical properties of electrodeposited Ni−Co alloy [J]. Transactions of Nonferrous Metals Society of China, 2016, 26: 484−491.

[7] SYUKRI, BAN T, OHYA Y, TAKAHASHI Y. A simple synthesis of metallic Ni and Ni–Co alloy fine powders from a mixed-metal acetate precursor [J]. Material Chemistry and Physics, 2003, 78: 645−649.

[8] MATTEI G, de JULIÁN FERNÁNDEZ C, MAZZOLDI P, SADA C, DE G, BATTAGLIN G, SANGREGORIO C, GATTESCHI D. Synthesis, structure, and magnetic properties of Co, Ni, and Co−Ni alloy nanocluster-doped SiO_2 films by sol−gel processing [J]. Chemistry of Materials, 2002, 14: 3440−3447.

[9] ZHAN Jing, ZHOU Di-fei, ZHANG Chuan-fu. Shape-controlled synthesis of novel precursor for fibrous Ni−Co alloy powders [J]. Transactions of Nonferrous Metals Society of China, 2011, 21: 544−551.

[10] CHENG M, WEN M, ZHOU S, WU Q, SUN B. Solvothermal synthesis of NiCo alloy icosahedral nanocrystals [J]. Inorganic Chemistry, 2012, 51: 1495−1500.

[11] ZHAN Jing, HE Yue-hui, ZHOU Di-fei, ZHANG Chuan-fu. Thermodynamic analysis on synthesis of fibrous Ni−Co alloys precursor and Ni/Co ratio control [J]. Transactions of Nonferrous Metals Society of China, 2011, 21: 1141−1148.

[12] POPOV K I, DJOKIĆ S S, NIKOLIĆ N D, JOVIĆ V D. Morphology of electrochemically and chemically deposited metals [M]. New York: Springer, 2016.

[13] PLOWMAN B J, JONES L A, BHARGAVA S K. Building with bubbles: The formation of high surface area honeycomb-like films via hydrogen bubble templated electrodeposition [J]. Chemical Communications, 2015, 51: 4331−4346.

[14] WINAND R. Electrodeposition of metals and alloys—New results and perspectives [J]. Electrochimica Acta, 1994, 39: 1091−1105.

[15] NIKOLIĆ N D, POPOV K I, PAVLOVIĆ L J, PAVLOVIĆ M G. The effect of hydrogen codeposition on the morphology of copper electrodeposits. I: The concept of effective overpotential [J]. Journal of Electroanalytical Chemistry, 2006, 588: 88−98.

[16] NIKOLIĆ N D, PAVLOVIĆ Lj J, PAVLOVIĆ M G, POPOV K I. Formation of dish-like holes and a channel structure in electrodeposition of copper under hydrogen co-deposition [J]. Electrochimica Acta, 2007, 52: 8096−8104.

[17] SHIN H C, DONG J, LIU M L. Nanoporous structures prepared by an electrochemical deposition process [J]. Advanced Materials, 2003, 15: 1610−1614.

[18] SHIN H C, LIU M L. Copper foam structures with highly porous nanostructured walls [J]. Chemistry of Materials, 2004, 16: 5460−5464.

[19] LI Ying, JIA Wen-zhi, SONG Yan-yan, XIA Xing-hua. Superhydrophobicity of 3D porous copper films prepared using the hydrogen bubble dynamic template [J]. Chemistry of Materials, 2007, 19: 5758−5764.

[20] CHEREVKO S, XING X, CHUNG C H. Electrodeposition of three-dimensional porous silver foams [J]. Electrochemistry Communication, 2010, 12: 467−470.

[21] CHEREVKO S, CHUNG C H. Direct electrodeposition of nanoporous gold with controlled multimodal pore size distribution [J]. Electrochemistry Communication, 2011, 13: 16−19.

[22] YU Xiang-tao, WANG Ming-yong, WANG Zhi, GONG Xu-zhong, GUO Zhan-cheng. The structure evolution mechanism of electrodeposited porous Ni films on NH_4Cl concentration [J]. Applied Surface Science, 2016, 360: 502−509.

[23] CHEREVKO S, KULYK N, CHUNG C H. Nanoporous palladium with sub-10 nm dendrites by electrodeposition for ethanol and ethylene glycol oxidation [J]. Nanoscale, 2012, 4: 103−105.

[24] OTT A, JONES L A, BHARGAVA S K. Direct electrodeposition of porous platinum honeycomb structures [J]. Electrochemistry Communication, 2011, 13: 1248−1251.

[25] SHIN H C, LIU M L. Three-dimensional porous copper−tin alloy electrodes for rechargeable lithium batteries [J]. Advanced Functional Materials, 2005, 15: 582−586.

[26] EUGÉNIO S, SILVA T M, CARMEZIM M J, DUARTE R G, MONTEMOR M F. Electrodeposition and characterization of nickel–copper metallic foams for application as electrodes for supercapacitors [J]. Journal of Applied Electrochemistry, 2014, 44: 455−465.

[27] RAFAILOVIĆ L D, GAMMER C, RENTENBERGER C, KLEBER C, WHITEHEAD A H, GOLLAS B, KARNTHALER H P. Preparation of CoNi high surface area porous foams by substrate controlled electrodeposition [J]. Physical Chemistry Chemical Physics, 2012, 14: 972−980.

[28] NIKOLIĆ N D, PAVLOVIĆ L J, PAVLOVIĆ M G, POPOV K I. Morphologies of electrochemically formed copper powder particles and their dependence on the quantity of evolved hydrogen [J]. Powder Technology, 2008, 185: 195−201.

[29] NIKOLIĆ N D, AVRAMOVIĆ L, IVANOVIĆ E R, MAKSIMOVIĆ V M, BAŠČAREVIĆ Z, IGNJATOVIĆ N. Comparative morphological and crystallographic analysis of copper powders obtained under different electrolysis conditions [J]. Transactions of Nonferrous Metals Society of China, 2019, 29: 1275−1284.

[30] AVRAMOVIĆ L, MAKSIMOVIĆ V M, BAŠČAREVIĆ Z, IGNJATOVIĆ N, BUGARIN M, MARKOVIĆ R, NIKOLIĆ N D. Influence of the shape of copper powder particles on the crystal structure and some decisive characteristics of the metal powders [J]. Metals, 2019, 9: 56.

[31] JOVIĆ V D, JOVIĆ B M, PAVLOVIĆ M G. Electrodeposition of Ni, Co and Ni−Co alloy powders [J]. Electrochimica Acta, 2006, 51: 5468−5477.

[32] JOVIĆ V D, JOVIĆ B M, PAVLOVIĆ M G, MAKSIMOVIĆ V. Morphology and composition of Ni−Co alloy powders electrodeposited from ammoniacal electrolyte [J]. Journal of Solid State Electrochemistry, 2006, 10: 959−966.

[33] MAKSIMOVIĆ V M, LAČNJEVAC U Č, STOILJKOVIĆ M M, PAVLOVIĆ M G, JOVIĆ V D. Morphology and composition of Ni−Co electrodeposited powders [J]. Materials Characterization, 2011, 62: 1173−1179.

[34] RAFAILOVIĆ L D, MINIĆ D M, KARNTHALER H P, WOSIK J, TRIŠOVIĆ T, NAUER G E. Study of the dendritic growth of Ni−Co alloys electrodeposited on Cu substrates [J]. Journal of the Electrochemical Society, 2010, 157: D295−D301.

[35] RAFAILOVIĆ L D, KARNTHALER H P, TRIŠOVIĆ T, MINIĆ D M. Microstructure and mechanical properties of disperse Ni−Co alloys electrodeposited on Cu substrates [J]. Materials Chemistry and Physics, 2010, 120: 409−416.

[36] SILVA R P, EUGÉNIO S, SILVA T M, CARMEZIM M J, MONTEMOR M F. Fabrication of three-dimensional dendritic Ni−Co films by electrodeposition on stainless steel substrates [J]. The Journal of Physical Chemistry C, 2012, 116: 22425−22431.

[37] SPASOJEVIĆ M, SPASOJEVIĆ M, MAŠKOVIĆ M, MARKOVIĆ D, RIBIĆ-ZELENOVIĆ L. Electrodeposition, microstructure and magnetic properties of nickel−cobalt−copper alloy powders [J]. Journal of the Electrochemical Society, 2018, 165: D511−D517.

[38] WANG Li-ping, GAO Yan, XUE Qun-ji, LUI Hui-wen, XU Tao. Microstructure and tribological properties of electro-deposited Ni−Co alloy deposits [J]. Applied Surface Science, 2005, 242: 326−332.

[39] BRENER A. Electrodeposition of alloys: Principles and practice [M]. New York: Academic, 1963.

[40] KRAUS W, NOZLE G. Powder cell−A program for the representation and manipulation of crystal structures and calculation of the resulting X-ray powder patterns [J]. Journal of Applied Crystallography, 1996, 29: 301−303.

[41] DOWNS R T, HALL-WALLACE M. The american mineralogist crystal structure database [J]. American Mineralogist, 2003, 88: 247−250.

[42] CHEN Lin, ZHU Qing-shan, WU Rong-fang. Effect of Co−Ni ratio on the activity and stability of Co−Ni bimetallic aerogel catalyst for methane Oxy−CO_2 reforming [J]. International Journal of Hydrogen Energy, 2011, 36: 2128−2136.

[43] RASHID M H, RAULA M, MANDAL T K. Polymer assisted synthesis of chain-like cobalt−nickel alloy nanostructures: Magnetically recoverable and reusable catalysts with high activities [J]. Journal of Materials Chemistry, 2011, 21: 4904−4917.

[44] WU B Y C, FERREIRA P J, SCHUH C A. Nanostructred Ni−Co alloys with tailorable grain size and twin density [J]. Metallurgical and Materials Transactions A, 2005, 36: 1927−1936.

[45] JOVIĆ V D, TOŠIĆ N, STOJANOVIĆ M. Characterization of electrodeposited Co+Ni alloys by application of the ALSV [J]. Journal of Electroanalytical Chemistry, 1997, 420: 43−51.

[46] ABD EL-HALIM A M. Apparent equilibrium codeposition of Ni−Co alloy powder from dilute sulphate baths [J]. Surface and Coatings Technology, 1987, 30: 183−190.

[47] ELUMALAI P, VASAN H N, VERELST M, LECANTE P, CARLES V, TAILHADES P. Synthesis and characterization of sub-micron size Co−Ni alloys using malonate as precursor [J]. Materials Research Bulletin, 2002, 37: 353−363.

[48] OES A, KAZAR F, KUCAB M, SIKORA W. Magnetic structures [M]. Krakow: National Scientific Publishing House, 1976.

[49] CRAIK D. Magnetism: Principles and applications [M]. New York: John Wiley & Sons, 1995.
[50] NIKOLIĆ N D, BRANKOVIĆ G, MAKSIMOVIĆ, V M. Morphology and internal structure of copper deposits electrodeposited by the pulsating current regime in the hydrogen co-deposition range [J]. Journal of Solid State Electrochemistry, 2012, 16: 321−328.
[51] NIKOLIĆ N D, BRANKOVIĆ G, PAVLOVIĆ M G. Correlate between morphology of powder particles obtained by the different regimes of electrolysis and the quantity of evolved hydrogen [J]. Powder Technology, 2012, 221: 271−277.

电解液中 Ni^{2+}/Co^{2+}比对电解 Ni−Co 合金粉末形貌、结构和磁学性能的影响

Vesna M. MAKSIMOVIĆ[1], Vladan B. KUSIGERSKI[1],
Milovan M. STOILJKOVIĆ[1], Jelena R. MALETAŠKIĆ[1,2], Nebojša D. NIKOLIĆ[3]

1. Institute of Nuclear Sciences, “Vinča”, University of Belgrade, P. O. Box 522, Belgrade 11001, Serbia;
2. Laboratory for Advanced Nuclear Energy, Institute of Innovative Research,
Tokyo Institute of Technology, 2-12-1 Ookayama, Meguro-ku, Tokyo 152-8550, Japan;
3. ICTM-Department of Electrochemistry, University of Belgrade,
Njegoševa 12, P. O. Box 473, Belgrade 11001, Serbia

摘　要：采用恒电流法在具有不同 Ni^{2+}/Co^{2+}比(摩尔比)的硫酸盐电解液中制备镍钴(Ni−Co)合金粉末。利用扫描电镜(SEM)、X 射线衍射仪(XRD)、原子发射光谱仪(AES)和基于 SQUID 的磁力仪检测粉末的形态、相结构、化学成分和磁学性能。当 Ni^{2+}/Co^{2+}比从 0.25 增加到 4.0 时，颗粒形貌从菜花状和树枝状转变为珊瑚状和海绵状。Ni−Co 粉末的 XRD 分析表明，Ni/Co 比降低(Co 含量增加)导致结构变化：Ni^{2+}/Co^{2+}比为 4.0、1.5 和 0.67 时，粉末为面心立方(FCC)结构；Ni/Co 比为 0.25 时，粉末为面心立方(FCC)和六方密堆(HCP)相的混合物。增加电解液中 Ni 含量导致电解机理发生变化：当电解液中 Ni 含量低于 40%(质量分数)时为不规则共沉积；Ni 含量为 40%~60%(质量分数)时接近平衡共沉积，Ni 含量高于 60%(质量分数)时则为异常共沉积。所有获得的 Ni−Co 合金样品均为软磁材料，其磁性参数显示出直接的成分依赖性，因为矫顽力和饱和磁化强度几乎都随 Co 含量线性增大。

关键词：Ni−Co 合金粉末；电解；氢；形貌；磁学性能

(Edited by Wei-ping CHEN)